



## Oxovanadium (IV) Dipicolinate: Structure Nucleolytic and Anticancer Property

Teoh Siang Guan (Corresponding author)

School of Chemical Science, Universiti Sains Malaysia, 11800 Minden,  
Penang, Malaysia

Tel : +6016- 4510177 E-mail: ppskl@yahoo.com or sgteoh@usm.my

Ng Chew Hee

Faculty of Engineering and Science, Universiti Tunku Abdul Rahman, 53100 Kuala Lumpur, Malaysia

Tel : 603-41079802 E-mail: ngch@mail.utar.edu.my

Tarn Fang Lai

Faculty of Engineering and Science, Universiti Tunku Abdul Rahman, 53100 Kuala Lumpur, Malaysia

Lim Eng Khoon

School of Chemical Science, Universiti Sains Malaysia, 11800 Minden,  
Penang, Malaysia

Tel : +6016-4164478 E-mail: chemistlim@yahoo.com

Sharif Mahsufi Mansor

Centre for Drug Research, 11800 Penang, Universiti Sains Malaysia;

Pauline Balraj

Molecular Pathology Unit, Institute for Medical Research, 50588 Kuala Lumpur, Malaysia

Tai Lin Chu

Molecular Pathology Unit, Institute for Medical Research, 50588 Kuala Lumpur, Malaysia

Bohari M. Yamin

School of Chemical Science and Food Technology, Universiti Kebangsaan Malaysia, 43600 Bangi, Selangor, Malaysia

Tel : +6016-6587435 E-mail: bohari\_nor@yahoo.com.my

Seik Weng Ng

Department of Chemistry, University of Malaya, 50603 Kuala Lumpur, Malaysia

*We like would like to thank the Malaysian Academy of Science and Ministry of Science, Technology and Innovation for the SAGA grant which was used to finance this research*

### Abstract

Diaqua(dipicolinato)oxovanadium (IV) ethanol solvate crystallizes in the triclinic space group  $P1$ . The complex was characterized by FTIR, elemental analysis, thermal gravimetric analysis, and solution visible spectral analysis. The complex alone cleaved DNA in the absence of hydrogen peroxide and its nucleolytic efficiency is greater than that of  $\text{VO}_2$ . Its nucleolytic efficiency is affected by the choice of buffer used and pH. DNA cleavage can be inhibited by DMSO,  $\text{NaN}_3$  and catalase, implying involvement of ROS. An MTT assay, involving the lung cancer cell line PC9, gave  $\text{IC}_{50}$  values of 9.5  $\mu\text{M}$  and 16  $\mu\text{M}$  for the complex and  $\text{VO}_2$  respectively. For breast cancer cell line MCF-7, this complex is less cytotoxic, with an  $\text{IC}_{50}$  of 16  $\mu\text{M}$ .

**Keywords:** Oxovanadium(IV) complex, Dipicolinic acid, Crystal structure, DNA cleavage, Anticancer

### 1. Introduction

Vanadium(IV) and vanadium(V) inorganic salts and complexes have generated widespread interest due its insulin-mimetic property [Crans, *et al.*, 2000, Sakurai, *et al.*, 2002, Shechter, *et al.*, 2003]. In the search for a better and less toxic oral substitute for insulin in the treatment of both Type I and Type II diabetes, vanadium complexes of newer

organic ligands have been synthesized. Among them, the vanadium (IV) and vanadium (V) complexes of dipicolinic acid and derivatives have been found to be insulin-mimetic [Crans, *et al.*, 2000, 2003]. Besides this insulin-mimetic property, some vanadium salts and complexes have been investigated for their antitumor behaviour and their possible development into a new class of non-platinum antitumor agents [Evangelou, 2002]. Here, Evangelou reported that DNA cleavage *in vivo* and *in vitro* was shown to be among one of the different modes of action of these antitumor vanadium compounds. This paper presents the crystal structure of a *diaqua* (dipicolinato)oxovanadium(IV) ethanol solvate, abbreviated as VO(dipic), and both its nucleolytic and anticancer properties.

## 2. Experimental

### 2.1 Reagents, methods and instrumentation

All chemicals purchased were of reagent grade and were used without further purification. Ethanol, concentrated hydrochloric acid, sodium azide, dimethyl sulfoxide (DMSO) and catalase were used as received. Supercoiled plasmid pBR322 was purchased from BioSynTech (Fermentas). Elemental analysis was performed using a Perkin Elmer 2400 CHN/O analyzer series-11. Infrared spectra (KBr pellets) were recorded using a Perkin-Elmer 2000 Infrared Spectrometer. The UV-visible was obtained from a Hitachi U-2000 spectrophotometer. The electrophoresis experiments were performed on a horizontal gel electrophoresis system.

### 2.2 Synthesis of VO(dipic)

A mixture of V<sub>2</sub>O<sub>5</sub> (1.00g, 5.50 mmol), ethanol, concentrated hydrochloric acid and distilled water in a total volume of 20 ml was heated until all V<sub>2</sub>O<sub>5</sub> dissolved. A solution prepared from dipicolinic acid (also called pyridine-2,6-dicarboxylic; 1.01g, 6.05 mmol) and NaOH (0.24 g, 6.05 mmol) in a small volume of water was then added to the vanadium solution. The mixture was heated for another 3 hours. The pH of the resultant mixture was adjusted to 2.5-2.7 with Na<sub>2</sub>CO<sub>3</sub> solution. The dark green solution was then allowed to cool down to room temperature. Green crystals were obtained on cooling the solution overnight. Yield 0.91g (28.4 % based on V). Elemental analysis: found C, 32.71; H, 3.68; N, 4.38 %. Calculated for [VO(C<sub>7</sub>H<sub>3</sub>NO<sub>4</sub>)(H<sub>2</sub>O)<sub>2</sub>]. 0.5 CH<sub>3</sub>CH<sub>2</sub>OH: C, 33.00; H, 3.46; N, 4.81 %. IR (KBr): 3160vs, 1670vs, 1598s, 1434m, 1350vs, 1258m, 1177s, 1141m, 1095w, 1071s, 1048s, 1033m, 972vs, 924m, 855w, 831w, 772s, 750s, 683s, 591w, 490w, 459s cm<sup>-1</sup>.

### 2.3 Crystal structure determination

Diffraction data was collected on a Bruker APEX CCD area-detector diffractometer at 295 K on a crystal of size 0.50 x 0.46 x 0.26 mm using the  $\omega$ -scan technique over the range  $2.0 < \theta < 25.0^\circ$  equipped with Mo K $\alpha$  radiation ( $\lambda = 0.71073 \text{ \AA}$ ). The intensity data was collected over the range  $\theta = 2.0 - 25.0^\circ$  for 3676 reflections. Lorentz-polarization and absorption corrections were applied. Crystal structure data and refinement are tabulated in table 1. The structure was solved and refined by using SHELX system of programs [Sheldrick, 1997]. The final  $R$  ( $F^2 > 2\sigma(F^2)$ ) and  $R_w(F^2)$  values were 0.035 and 0.094. The water H atoms were located and refined. The ethanol molecule is disordered over two sites, and was refined with distance restraints. All non-hydrogen atoms were refined anisotropically. The hydrogen atoms were treated by a mixture of independent and constrained refinement. The weighting scheme was  $w = 1/[\sigma^2(F_o^2) + (0.0548 P)^2 + 0.5286 P]$  where  $P = (F_o^2 + 2F_c^2)/3$ . The perspective view of the molecule was obtained using ORTEP [Johnson, 1976]. Selected bond distances and angles are listed in table 2. Detailed crystallographic data for the crystal structure analysis have been deposited with the Cambridge Crystallographic Data Center, CCDC No. 604153.

### 2.4 Electrophoresis

Agarose gel electrophoresis experiments were carried out on supercoiled plasmid DNA pBR322 (4.4 kb) using a horizontal gel system. For each experiment, a 20  $\mu$ L mixture consisting of the appropriate volumes of stock solutions of DNA, complex dissolved in Tris-NaCl buffer pH 7 (100 mM Tris, 150 mM NaCl; abbreviated as TN buffer; Tris = Tris(hydroxymethyl)aminomethane; EDTA = disodium salt of ethylenediaminetetraacetic acid) buffer. The nucleolytic experiment was repeated in phosphate buffer at pH 7.5. The effect of ROS radical scavengers DMSO (.OH), catalase (peroxide species and superoxide radical anion) and sodium azide (singlet oxygen) on the nucleolytic activity of VO(dipic) was also investigated. Each 20  $\mu$ L mixture in experiments involving scavengers was similarly prepared. All samples were incubated at 37  $^\circ$ C for 1 or 4 h, and then electrophoresed on 1% agarose gel for 2 - 3 h at 80V. Essentially, 0.0125 mg mL<sup>-1</sup> DNA samples were incubated with the complex with or without the scavenger. The resultant DNA bands were stained with ethidium bromide before being photographed under UV light using a Syngene Bio Imaging system and the image was viewed with Gene Flash software.

### 2.5 MTT assay

The human lung adenocarcinoma cell line, PC9 used in this study was obtained from American Type Culture Collection. The cells were grown in RPMI 1640 supplemented with 10% FCS, 0.025 M Hepes, 0.024 M sodium bicarbonate, 50 units/ml penicillin G/streptomycin sulfate at 37  $^\circ$ C in 5% CO<sub>2</sub>. All tissue culture reagents were obtained from Sigma and Life Technologies Inc., Gaithersburg, MD. Cell line was cultivated for a minimum of two passages after thawing prior to

experimentation. The oestrogen receptor positive human breast adenocarcinoma cell line MCF-7 was also similarly tested. MTT assay was used to test the antiproliferative property of VO(dipic) against both cell lines. Additionally for PC9, the precursor VOSO<sub>4</sub> was also evaluated to compare the effect of chelating the dipicolic acid to the oxovanadium(IV). Exponentially growing PC9 tumour cells were seeded into a 96-well plate at a density of  $9 \times 10^4$  cells/well and incubated in a medium containing the vanadium compounds at concentration ranging from 1.6 – 240  $\mu$ M for 72 h at 37 °C in humidified 5% CO<sub>2</sub> atmosphere. For the MCF-7 tumor cells, 0.25% trypsin EDTA solution was used to detach the cells from the surface, and the concentration of VO(dipic) used varies from 1.9 – 1000  $\mu$ M. Every experiment was conducted on triplicate wells. Into each well 20  $\mu$ l of MTT (5mg/ml) was added. The plates were then incubated at 37 °C for 4 h to allow MTT to form formazan crystals. The crystals were then solubilized using DMSO for a few minutes. The absorbance of each well was measured in a microplate reader Dynatech MRX at 570 nm with a reference wavelength of 630 nm. The percentage of cell viability was calculated with the formula: Average A570 value for live cell (test) / average A570 value for live cell (control) x 100. The IC<sub>50</sub> values were obtained from the graphs drawn.

### 3. Results and discussion

#### 3.1 Structure analysis

The ORTEP plot of the complex (Fig. 1) shows the structure of the complex together with the lattice ethanol molecule (which is disordered). The dipicolinate anion coordinates to the VO<sup>2+</sup> cation as a tridentate ligand *via* two carboxylate oxygen atoms and its pyridyl nitrogen atom such that the carboxylate oxygen atoms are *trans* to each other while the pyridyl nitrogen atom is *trans* to the oxo atom of the VO<sup>2+</sup> cation. The non-hydrogen atoms of both the dipicolinate and oxovanadium (IV) moieties are coplanar. The coordinated water molecules are *trans* to each other; they are roughly perpendicular to the ‘dipicolinate-V=O’ plane and have the appearance of the two wings of a spaceship as they are slightly bent inwards towards the pyridyl nitrogen atom. Thus, the vanadium atom has a distorted octahedral geometry. The structure of the present diaqua(dipicolinato)oxovanadium(IV) complex is the same as that of previously determined dihydrate and tetrahydrate species [Yong, *et al.*, 2004, Chatterjee, *et al.*, 1999 and Bersted *et al.* 1968]. The only difference is that our complex has ethanol molecules instead of water molecules in the crystal lattice, and this leads to a slight difference in the hydrogen bonding network. The ethanol molecule is disordered over two sites in a 1:1 ratio but the two moieties share a common hydroxyl group. Two adjacent diaqua(dipicolinato)oxovanadium(IV) molecules in the same unit cell are hydrogen-bonded to each other *via* bonding between coordinated O2w atom (proton donor) of one complex molecule to the carboxylate oxygen atom O3 (proton acceptor) of the other complex molecule; there are thus two such intermolecular hydrogen bonds. Hydrogen bonds involving coordinated water molecules (O2w, O1w), carbonyl and carboxylate oxygen atoms (O1, O2, O3, O4) and the ethanol oxygen atom (O6) link the diaqua(dipicolinato)oxovanadium(IV) and ethanol molecules in the crystal lattice into a three-dimensional network (Fig. 2). The difference in V-O (carboxylate oxygen atom) bond length observed (V1-O1 = 2.031; V1-O3 = 2.053 Å) may be ascribed to difference in the proton donors (O1···H-O6 of ethanol molecule) and (O3···H-O2w of coordinated water molecule). The above H-bonding network is reflected in the higher temperature for the onset of the first stage of the thermal degradation of the complex. The first stage occurs over the range 125.0 - 270.0 °C, and this corresponds to the loss of coordinated water and ethanol molecules. The total weight loss is 30.0 % which is in close agreement with the calculated value of 28.2 %. However, the DTG spectrum seems to be able to distinguish the loss of these molecules as there are three endothermic peaks at 157.1 °C, 167.6 °C and 195.1 °C. The second stage of the degradation occurs over the range of 360.0 - 620.0 °C and it has an endothermic peak (DTG signal) at 474.2 °C. This may be ascribed to partial decomposition of dipicolinate ligand as the weight loss is only 24.0 %. A black residue is obtained at 800 °C. As this paper presents the biomedical property of VO (dipic) solution, the electronic spectral data of its solution was also obtained. The solution of the present complex in Tris-NaCl (TN) buffer pH 7 has a  $\lambda_{\text{max}}$  of 830 nm ( $\epsilon$ , 28 M<sup>-1</sup> cm<sup>-1</sup>) in the visible region and this is slightly different from that value ( $\sim$ 11.2 kK,  $\sim$ 880 nm) which was previously obtained for the VO(dipic) tetrahydrate in Nujol mull [Bersted *et al.* 1968]. There is also a shoulder at 620 nm ( $\epsilon$ , 21 M<sup>-1</sup> cm<sup>-1</sup>). Dissolving the complex in water shows no appreciable change in its  $\lambda_{\text{max}}$  value which is 844 nm ( $\epsilon$ , 34 M<sup>-1</sup> cm<sup>-1</sup>) and a shoulder at 626 nm ( $\epsilon$ , 17 M<sup>-1</sup> cm<sup>-1</sup>), suggesting no change in coordination sphere of the complex in both media. In contrast, the spectrum of VOSO<sub>4</sub> in TN buffer has a  $\lambda_{\text{max}}$  of 763 nm ( $\epsilon$ , 15 M<sup>-1</sup> cm<sup>-1</sup>) and a shoulder at 610 nm ( $\epsilon$ , 12 M<sup>-1</sup> cm<sup>-1</sup>). The spectrum of VOSO<sub>4</sub> in water also shows no appreciable change in the corresponding  $\lambda_{\text{max}}$  values, viz. 765 nm ( $\epsilon$ , 13 M<sup>-1</sup> cm<sup>-1</sup>) and 610 nm ( $\epsilon$ , 5 M<sup>-1</sup> cm<sup>-1</sup>). When the complex was dissolved in phosphate buffer pH 7 instead of TN buffer pH 7, the position of the two observed bands in the visible region seems unchanged. However, the intensity of these bands is about ten times higher in phosphate buffer. The increase in intensity was even more pronounced when the pH of the buffer was increased to pH 7.5 (Table 3). Similar trends are observed for the charge transfer bands for the complex dissolved in TN and phosphate buffers.

#### 3.2 DNA cleavage and MTT assay

##### 3.2.1 DNA cleavage by VO(dipic)

Agarose gel electrophoresis was used to study the cleavage of supercoiled plasmid DNA pBR322 (4361 bp) by the complex. The complex, at 50  $\mu$ M, is able to induce small amount of single strand cleavage of the DNA in TN buffer at pH

7 (Fig. 3, lane 4). DNA cleavage increases with increasing concentration of the complex. At about 3 mM, a linear band of DNA is observed, and this arises due to double-strand cleavage. Although double-strand break is dangerous due to possible apoptosis, direct inactivation of key genes, or consequential serious chromosomal aberrations [Barzilai *et al.*, 2004], such cellular concentration level may not be normally reached. When the DNA is incubated with 6 mM of complex, almost complete conversion of supercoiled pBR322 to both nicked and linear DNA occurs. In contrast, the starting material  $\text{VO}_2^+$  does not seem to cleave the DNA at 6 mM (Fig. 3, lane 11). Complexation of dipicolinic acid to the  $\text{VO}^{2+}$  enhances its nucleolytic property. This result contrasts with previous studies of DNA cleavage by other oxovanadium(IV) complexes where hydrogen peroxide is needed and reactive  $\cdot\text{OH}$  radicals are involved [Evangelou, 2002, Sakurai *et al.*, 1995, 1994]. The above cleavage may be due to the reaction of the VO (dipic) complex with molecular oxygen to yield oxygen-derived radical species. A previous report mentioned that vanadium (IV) could generate  $\text{O}_2\cdot^-$  and subsequently produced peroxovanadyl [ $\text{V}(\text{IV})\text{-OO}\cdot$ ] and vanadyl hydroperoxide [ $\text{V}(\text{IV})\text{-OH}\cdot$ ] radicals [Valko *et al.*, 2006]. Binding of molecular oxygen to a vanadium (IV) complex and subsequent one electron transfer was postulated to yield a very reactive  $\text{V}(\text{V})\text{-OO}\cdot$  radical species [Kotchevar *et al.*, 2001]. Similar radical species may be involved in the DNA cleavage by VO (dipic) as no attempt was made to exclude dissolved oxygen. When the buffer was changed to phosphate pH 7.5, the VO (dipic) can nick the DNA at a lower concentration, i.e. 10  $\mu\text{M}$  (Fig. 4, lane 3) and shorter incubation time (1h). While 6 mM of the complex in TN buffer pH 7 was needed to convert most of the supercoiled DNA to both nicked and linear DNA, 1 mM of the complex in phosphate buffer at pH 7.5 could completely convert the supercoiled DNA to nicked and linear DNA (Fig. 4, lane 5). The increased nucleolytic efficiency may be partly attributed to relative quenching of ROS since it was previously found that Tris buffer could more efficiently scavenge  $\cdot\text{OH}$  radical than phosphate buffer [Hicks *et al.*, 1986]. The poorer scavenging effect of the phosphate buffer for the ROS produced in our experiment could help to explain the enhanced cleavage of DNA. Another contributing factor may be due to apparent increase in VO (dipic) species in phosphate buffer at pH 7.5 than those in TN buffer at pH 7. The  $\lambda_{\text{max}}$  of the UV-visible spectral bands of the complex in both TN and phosphate buffers at pH 7 and pH 7.5 are practically the same (Table 3). The higher molar absorptivity,  $\epsilon$ , of each band of the complex in phosphate buffer at pH 7.5 than the corresponding one in TN buffer at pH 7 suggests higher concentration of VO (dipic) species. Interestingly, increasing the concentration of the complex in the phosphate buffer from 1 mM to 6 mM did not cause increase in the extent of DNA cleavage. Inhibition of DNA cleavage by VO (dipic) was tested with various scavengers which are commonly used to quench the corresponding targeted radicals (Fig. 5). The results show that sodium azide (singlet oxygen scavenger), catalase (peroxide species scavenger) and DMSO (hydroxyl radical scavenger) can inhibit the DNA cleavage. Collectively, these results suggest the role of ROS in the DNA cleavage by VO(dipic). The cleavage mechanism is thus oxidative.

### 3.2.2 Cell viability assay

As some anticancer drugs act by targeting and degrading the DNA of the cancer cells, we have used MTT assay to screen the anticancer property of the VO (dipic) on two cancer cell lines. For the lung cancer cell line PC9,  $\text{IC}_{50}$  of the complex is 9.5  $\mu\text{M}$  while that for  $\text{VO}_2^+$  is 16  $\mu\text{M}$  (Fig. 6). Coordination of the dipicolinate ligand to the oxovanadium (IV) ion seems to enhance its anticancer property. Our results differ from a recent investigation into the cytotoxicity of three vanadium (III, IV, V)-dipicolinate complexes on Caco-2 cells gave their  $\text{IC}_{50}$  values at 1.8 mM [ $\text{V}^{\text{III}}\text{-dipic}$ ], 1.9 mM [ $\text{V}^{\text{IV}}\text{-dipic}$ = VO (dipic) reported in this paper] and 1.7 mM [ $\text{V}^{\text{V}}\text{-dipic}$ ] respectively [Zhang, *et al.*, 2006]. These values could not be correlated with the order of decreasing redox potential or of decreasing capacity to produce reactive oxygen and nitrogen species (RONS). Of relevant to our findings is that the [ $\text{V}^{\text{IV}}\text{O}(\text{dipic})(\text{H}_2\text{O})_2$ ]. $2\text{H}_2\text{O}$  used generated the least amount of RONS amongst the three vanadium-dipicolinate complexes and yet all these three complexes exhibited similar level of cytotoxicity. Our finding, in contrast, shows higher cytotoxicity using the same MTT assay. However, it is noted that the type of cells used is different. The VO (dipic) used may have a lower cytotoxicity to Caco-2 cells (which are originally derived from a human colorectal adenocarcinoma and are developed into a suitable model for the evaluation of intestinal absorption of drugs). Of relevance here is the fact that the  $\text{IC}_{50}$  values of these three vanadium-dipic complexes is similar to those obtained for *bis*(malonato)oxovanadium(IV), vanadyl acetylacetonate, and other vanadium (IV, V) complexes [Yang, *et al.* 2004, Rehder, *et al.* 2002]. It also seems reasonable to exclude the presence of ethanol solvate (some concentration as complex, i.e. 9.5  $\mu\text{M}$ ) as a factor in the higher toxicity of the present VO (dipic) complex towards PC9 cells as mM concentrations of ethanol have been found to promote cell growth of breast cancer cell line MCF-7 [DeCupis *et al.*, 1998, Przylipek, *et al.*, 1996, Izevbogie, *et al.* 2002]. When VO (dipic) was screened on the MCF-7 cancer cell line, its  $\text{IC}_{50}$  was slightly higher, at 16  $\mu\text{M}$ . Thus, this complex is very cytotoxic towards PC9 and MCF-7 cancer cells. Our nucleolytic experiments suggest that cell death may be due to cleavage or fragmentation of DNA of these cancer cells and that the active species responsible for this are ROS which resulted from the *in vitro* reaction of VO (dipic). However, this is not the only mechanism whereby vanadium compounds induce cell death [Ray, *et al.* 2006].

### References

Barzilai, A. & Yamamoto, K-I. (2004). DNA Repair, 3, pp.1109.

- Bersted, B. H., Belford, R. L. & Paul, I. C. (1968). *Inorg. Chem.* 7, pp.1557.
- Chatterjee, M. & Ghosh, S. (1999). *Transition Met. Chem.* 24, pp183
- Crans, D. C. (2000). *J. Inorg. Biochem.*, 80, pp. 123.
- Crans, D.C., Mohroof-Tahir, M., Johnson, M. D., Wilkins, P. C., Yang, L., Robbins, K., Johnson, A., Alfano, J. A., Godzala, M. E., Austin, L. T. & Willsky, G. R. (2003). *Inorg. Chim. Acta*, 356, pp 365.
- DeCupis, A., Pirani, P., Fazzuoli, L. & Favoni, R. E. (1998). *In Vitro Cell Dev. Biol.* 34 pp. 836.
- Evangelou, A. M. (2002). *Critical Rev. Oncology/Hematology*, 42, pp. 249.
- Hicks, M. & Gebiski, J. M. (1986). *FEBS Letters*, 199, pp. 3563.
- Izevbigie, E. B., Ekunwe, S. I., Jordan, J. & Howard, C. B. (2002). *Exp. Biol. Med.* 227, pp. 260.
- Johnson, C. K., (1976). *ORTEP-II*, Report ORNL-5138 (Oak Ridge National Laboratory, Oak Ridge, Tennessee, USA, 1976).
- Kotchevar, A. T., Ghosh, P., DuMex, D. D. & Uekun, F. M. (2001). *J. Inorg. Biochem.* 83, pp. 51.
- Przylipiak, A., Rabe, T., Hafner, J., Przylipiak, M. & Runnehaum, M. (1996). *Arch. GynecolObstet.* 258, pp.137.
- Ray, R. S., Rana, B., Swami, B., Venu, V. & Chatterjee, M. (2006). *Chemico-Biological Interactions*, 163, pp. 239.
- Rehder, D., Costa Pessoa, J., Geraldies, C. F., Castro, M. C., Kabanos, T., Kiss, T., Meier, B., Micera, G., Petterson, L., Rangel, M., Salifoglo, A., Turel, I. & Wang, D. (2002). *Inorg. Chem.* 7, pp. 384.
- Sakurai, H. (1994). *Envi. Health Perspect.* 3 pp. 35.
- Sakurai, H., Kojima, Y., Yoshikawa, Y., Kawabe, K. & Yasui, H. (2002). *Coord. Chem. Rev.*, 226, pp 187.
- Sakurai, H., Tamura, H. & Okatani, K. (1995). *Biochem. Biophys. Res. Commun.* 206, pp. 133
- Shechter, Y., Goldwasser, I., Mironchik, M., Fridkin, M. & Gefel, D. (2003). *Coord. Chem. Rev.*, 237, pp. 3.
- Sheldrick, G. M. (1997). *SHELX-97*, Programs for Crystal Structure Analysis (Release 97-2): (Göttingen University: Germany, 1997).
- Valko, M., Rhodes, C. J., Moncol, J., Izakovic, M. & Mazur, M. (2006) *Chemico-Biological Interactions* 160, pp 1.
- Yong, H. X., Katsuyuki, A. & Feng, Y. B. (2004). *J. Coord. Chem.* 57, pp157
- Yang, X. G., Yang, X. D., Yuan, L., Wang, K. & Crans, D. C. (2004) *Pharm. Res.* 21, pp.1026.
- Zhang, Y., Yang, X-D., Wang, K. and Crans, D. C. (2006). *J. Inorg. Biochem.*, 100, pp. 80.

Table 1. Crystal data and structure refinement

|                                                                             |                                                                |                                          |              |
|-----------------------------------------------------------------------------|----------------------------------------------------------------|------------------------------------------|--------------|
| Formula                                                                     | C <sub>9</sub> H <sub>13</sub> NO <sub>8</sub> V               | <i>a</i> (Å)                             | 6.7041(4)    |
| Formula weight                                                              | 314.14                                                         | <i>b</i> (Å)                             | 9.2664(5)    |
| Crystal system                                                              | Triclinic                                                      | <i>c</i> (Å)                             | 11.0221(7)   |
| Space group                                                                 | <i>P</i> 1                                                     | $\alpha$ (°)                             | 112.9610(10) |
| <i>V</i> (Å <sup>3</sup> )                                                  | 608.42(6)                                                      | $\beta$ (°)                              | 102.3640(10) |
| <i>D<sub>c</sub></i> (g cm <sup>-3</sup> )                                  | 1.715                                                          | $\gamma$ (°)                             | 93.1950(10)  |
| F(000)                                                                      | 322                                                            | T (K)                                    | 303(2)       |
| $\mu$ (mm <sup>-1</sup> )                                                   | 0.852                                                          | <i>Z</i>                                 | 2            |
| Index ranges                                                                | -7 ≤ <i>h</i> ≤ 6; -10 ≤ <i>k</i> ≤ 10;<br>-12 ≤ <i>l</i> ≤ 13 | $\lambda$ (Å)                            | 0.71073      |
| <i>R</i> [ <i>F</i> <sup>2</sup> > 2σ( <i>F</i> <sup>2</sup> )]             | 0.034                                                          | $\theta$ range (°)                       | 2.0, 25.0    |
| <i>R<sub>w</sub></i> [ <i>F</i> <sup>2</sup> > 2σ( <i>F</i> <sup>2</sup> )] | 0.094                                                          | Reflections refined                      | 2010         |
| <i>R</i> (all data)                                                         | 0.035                                                          | Goodness-of-fit on <i>F</i> <sup>2</sup> | 1.05         |
| <i>R<sub>w</sub></i> (all data)                                             | 0.094                                                          | <i>S</i>                                 | 1.05         |

Table 2. Selected geometric parameters

| Bond lengths and angles (Å, °) |          |              |            |
|--------------------------------|----------|--------------|------------|
| V1 - O5                        | 1.592(2) | O5-V1- O1w   | 99.20(10)  |
| V1 - O1w                       | 2.015(2) | O5-V1- O1    | 110.13(9)  |
| V1 - O1                        | 2.031(2) | O1w- V1- O1  | 86.27(7)   |
| V1 - O3                        | 2.053(2) | O5 - V1- O3  | 102.90(9)  |
| V1 - O2w                       | 2.080(2) | O1w -V1- O3  | 89.27(7)   |
| V1 - N1                        | 2.157(2) | O1- V1- O3   | 146.97(7)  |
| O1 - C1                        | 1.296(3) | O5-V1- O2w   | 93.70(9)   |
| O2 - C1                        | 1.223(3) | O1w- V1- O2w | 166.88(8)  |
| O3 - C7                        | 1.294(3) | O1- V1- O2w  | 87.10(7)   |
| O4 - C7                        | 1.224(3) | O3 - V1- O2w | 90.13(7)   |
| O6 - C8                        | 1.529(8) | O5 - V1- N1  | 174.38(9)  |
| O6 - C8'                       | 1.430(8) | O1w - V1- N1 | 84.97(8)   |
|                                |          | O1- V1- N1   | 73.75(7)   |
|                                |          | O3 -V1- N1   | 73.26(6)   |
|                                |          | O2w-V1-N1    | 82.32(7)   |
|                                |          | C1- O1-V1    | 122.68(14) |
|                                |          | C7- O3-V1    | 122.52(14) |

Table 3. Electronic spectral data of VO (dipic)

| Type of buffer & pH | d-d transition<br>$\lambda$ (nm), $\epsilon$ (cm <sup>-1</sup> M <sup>-1</sup> ) | Charge transfer band<br>$\lambda$ (nm), $\epsilon$ (cm <sup>-1</sup> M <sup>-1</sup> ) |
|---------------------|----------------------------------------------------------------------------------|----------------------------------------------------------------------------------------|
| Phosphate pH 7.5    | 836, 26                                                                          | 268, 5494                                                                              |
|                     | 616 (sh), 16                                                                     | 207, 18575                                                                             |
| TN pH 7.5           | 839, 25                                                                          | 267, 5081                                                                              |
|                     | 619 (sh), 12                                                                     | 214, 13516                                                                             |
| Phosphate pH 7      | 839, 4                                                                           | 269, 70                                                                                |
|                     | 615 (sh), 2                                                                      | 202, 310                                                                               |
| TN pH 7             | 840, 0.3                                                                         | 268, 72                                                                                |
|                     | 619 (sh), 0.2                                                                    | 209, 215                                                                               |

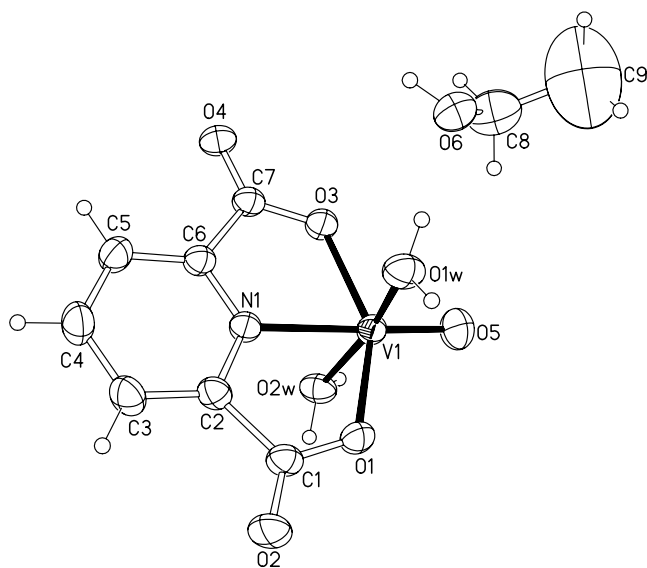


Figure 1. 50 % probability ORTEP plot of the VO (dipic) complex showing the lattice ethanol molecule

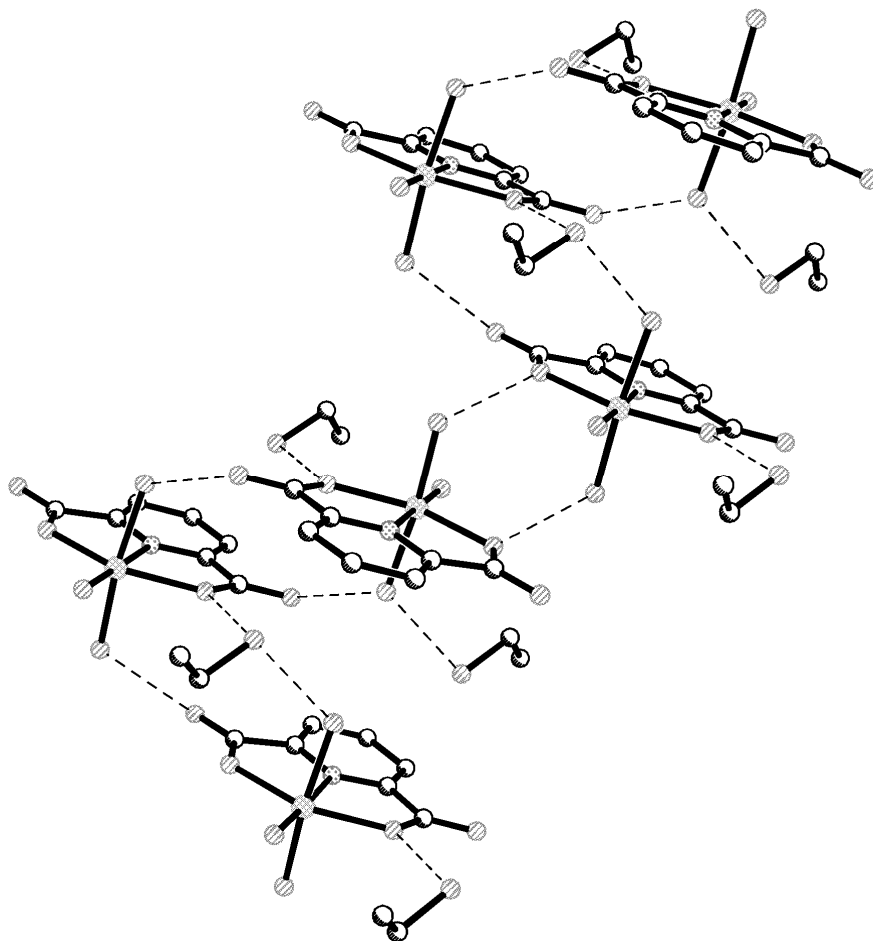


Figure 2. A view of the molecular packing of VO(dipic) complex showing the hydrogen Bonding interactions

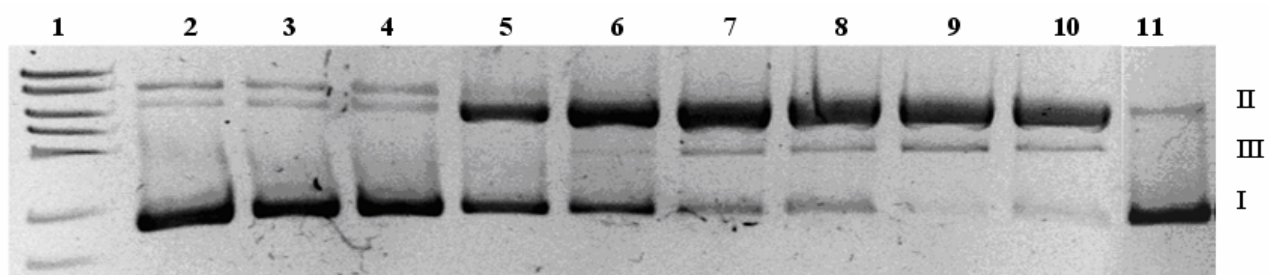


Figure 3. Cleavage of supercoiled pBR322 by VO(dipic) at different concentrations in TN buffer pH 7 incubated at 4 h.

Note: Lane 1, DNA ladder; and Lane 2, DNA alone. Lanes 3-10 DNA with increasing concentration of VO(dipic): lane 3, 10  $\mu$ M; lane 4, 50  $\mu$ M; lane 5, 1 mM; lane 6, 3 mM; lane 7, 4 mM; lane 8, 5 mM; lane 9, 5.5 mM; lane 10, 6 mM. Lane 11, 6 mM VOSO<sub>4</sub> in TN buffer pH 7. Form I, supercoiled DNA; Form II, supercoiled nicked; Form III, linear DNA.

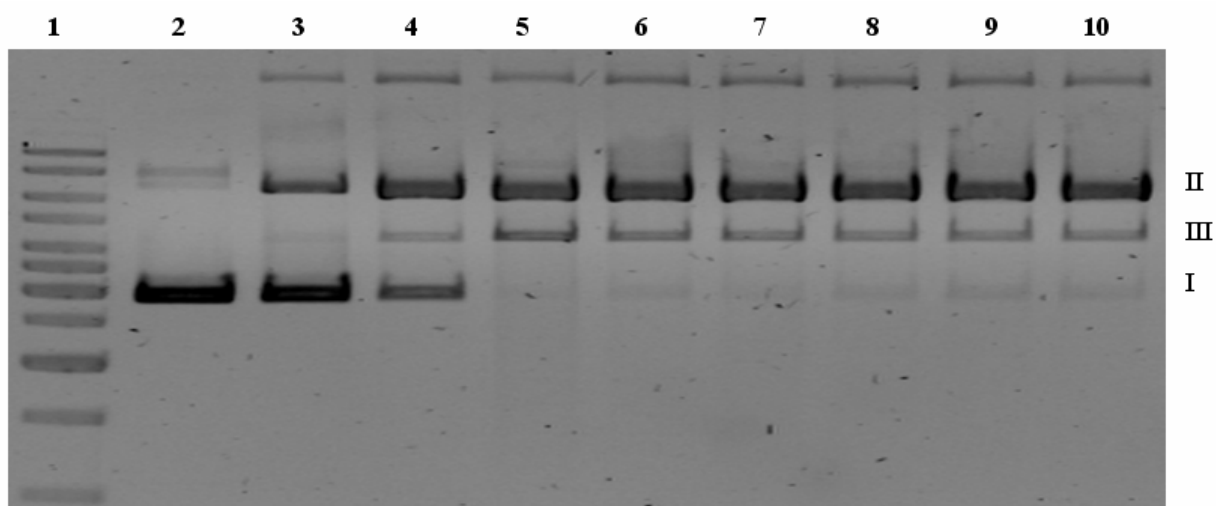


Figure 4. Cleavage of supercoiled pBR322 by VO(dipic) at different concentrations in phosphate buffer pH 7.5 with 1 h incubation time.

Note: Lane 1, DNA ladder; and Lane 2, DNA alone. Lanes 3-10 DNA with increasing concentration of VO(dipic): lane 3, 10  $\mu$ M; lane 4, 50  $\mu$ M; lane 5, 1 mM; lane 6, 3 mM; lane 7, 4 mM; lane 8, 5 mM; lane 9, 5.5 mM; lane 10, 6 mM. Form I, supercoiled DNA; Form II, supercoiled nicked; Form III, linear DNA



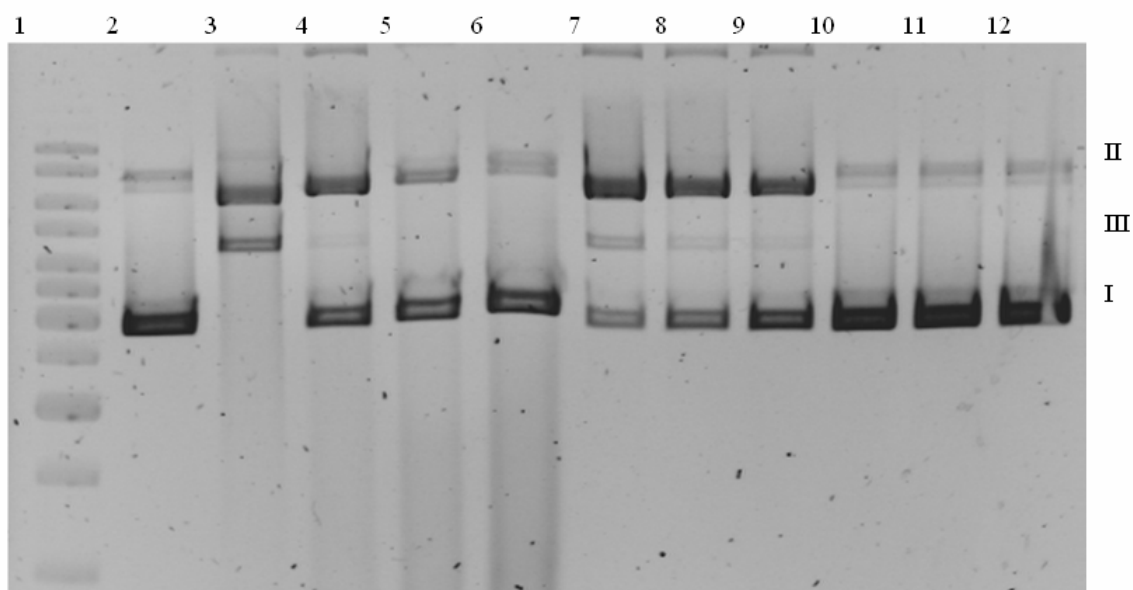


Figure 5. Effect of various scavengers on the cleavage of pBR322 (0.0125 mg mL<sup>-1</sup>) by 1 mM VO(dipic) in phosphate buffer pH 7.5 at 1 h incubation time.

Note: Lane 1, Gene Ruler 1 kb DNA ladder; lane 2, DNA alone; lane 3, DNA + 1 mM VO(dipic). Lanes 4 – 12 involves reaction of 1 mM complex with DNA in presence of various scavengers. Lanes 4 – 6: 1  $\mu$ L, 2  $\mu$ L, and 4  $\mu$ L catalase; lanes 7 – 9: 1 mM, 2 mM and 4 mM NaN<sub>3</sub>; lanes 10 – 12: 1  $\mu$ L, 2  $\mu$ L, and 4  $\mu$ L DMSO.

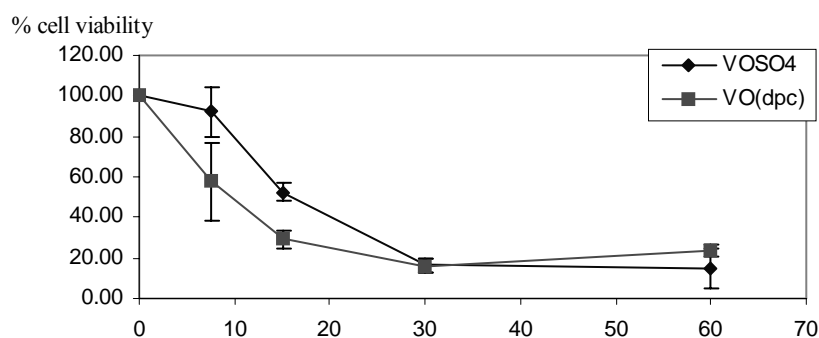


Figure 6. Cytotoxic activity of VOSO<sub>4</sub> and VO(dipic) against human lung adenocarcinoma PC9 cell line. Cancer cells were incubated at different concentration for 72 h in 96-well plates. Cell survival was determined using MTT assay. The average drug concentration needed to inhibit 50% of cell growth was obtained from pooled results from 3 different independent experiments.

% Cell viability

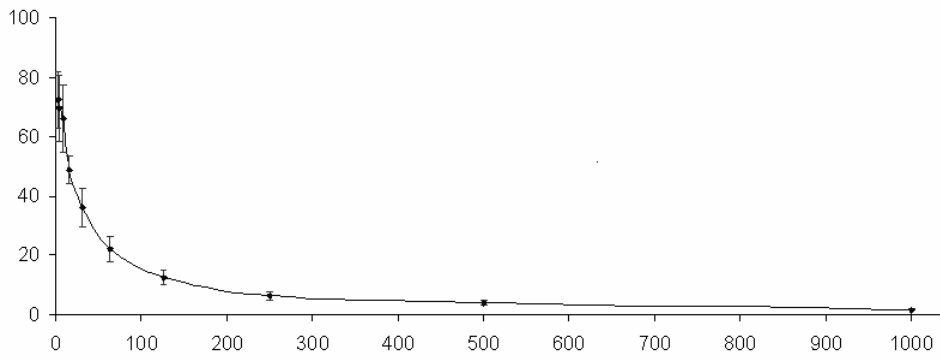


Figure 7. Cytotoxic activity of VO(dipic) against breast cancer MCF-7 cell line. Cancer cells were incubated at different concentrations for 72 h in 96-well plates.